

Strange Magnetism and the Anapole Structure of the Proton

R. Hasty², A. M. Hawthorne-Allen⁵, T. Averett⁹, D. Barkhuff⁴, D. H. Beck², E. J. Beise³,
A. Blake¹, H. Breuer³, R. Carr¹, S. Covrig¹, A. Danagoulian², G. Dodson⁴, K. Dow⁴,
M. Farkhondeh⁴, B. W. Filippone¹, J. Gao¹, M. C. Herda³, T. M. Ito¹, C. E. Jones¹,
W. Korsch⁶, K. Kramer⁹, S. Kowalski⁴, P. Lee¹, R. D. McKeown¹, B. Mueller⁷, M. Pitt⁵,
J. Ritter⁵, J. Roche⁹, V. Savu¹, D. T. Spayde³, R. Tieulent³, E. Tsentalovich⁴, S. P. Wells⁸,
B. Yang⁴, and T. Zwart⁴

¹ *Kellogg Radiation Laboratory, California Institute of Technology Pasadena, CA 91125, USA*

² *Department of Physics, University of Illinois at Urbana-Champaign, Urbana, Illinois 61801*

³ *Department of Physics, University of Maryland, College Park, Maryland 20742*

⁴ *Bates Linear Accelerator Center, Laboratory for Nuclear Science and Department of Physics,
Massachusetts Institute of Technology, Cambridge, Massachusetts 02139*

⁵ *Department of Physics, Virginia Polytechnic Institute and State University, Blacksburg, VA
24061-0435*

⁶ *Department of Physics and Astronomy, University of Kentucky, Lexington, KY 40506*

⁷ *Physics Division, Argonne National Laboratory, Argonne, IL 60439, USA*

⁸ *Department of Physics, Louisiana Tech University, Ruston, LA 71272, USA*

⁹ *Department of Physics, College of William and Mary, Williamsburg, VA 23187, USA*

The violation of mirror symmetry in the weak force provides a powerful tool to study the internal structure of the proton. Experimental results have been obtained that address the role of strange quarks in generating nuclear magnetism. The measurement reported here provides an unambiguous constraint on strange quark contributions to the proton's magnetic moment through the electron-proton weak interaction. We also report evidence for the existence of a parity-violating electromagnetic effect known as the anapole moment of the proton. The proton's anapole moment is not yet well understood theoretically, but it could have important implications for precision weak interaction studies in atomic systems such as cesium.

In 1933 the German physicist Otto Stern discovered that the magnetism of the proton was anomalously large, a factor of three larger than expected from the basic theory of quantum mechanics. This experiment turned out to be the first glimpse of the internal structure of the constituents of the atomic nucleus, and a tantalizing hint at the existence of quarks. Widespread applications of the proton’s magnetic properties, such as the magnetic resonance imaging (MRI) techniques used in biology and medicine, have been developed despite a lack of fundamental understanding of the basic dynamics that generates this magnetism. After the key discovery of internal structure in the proton in a high energy electron scattering experiment at the Stanford Linear Accelerator Center in the late 1960’s (1), the theory of Quantum Chromodynamics (QCD), which describes the interaction between quarks and the gluons that bind the quarks into the atomic nuclei observed in the periodic table, was developed. Despite almost 30 years of intense theoretical effort, QCD has been unable to produce numerical predictions for the basic properties of nucleons such as their degree of magnetism.

In 1988, Kaplan and Manohar (2) proposed that the study of the weak magnetic force (analogous to the usual magnetic force associated with electromagnetism) would allow a separation of the proton’s magnetism into the three contributing flavors of quarks: up, down and strange. Measuring the contribution from strange quark-antiquark pairs is of special interest because it relates directly to the “sea” of virtual quark-antiquark pairs in the proton, a phenomenon predicted by QCD. In 1989, it was noted that the weak magnetic force could be isolated using its unique property of lack of mirror symmetry, or parity violation (3). The basic idea was to study the preference for the proton’s interaction with electrons that have spin counterclockwise, over those with clockwise spin, relative to their direction of travel. We report data obtained using this method that, when combined with our previously published results (4,5), allow the first unambiguous determination of the proton’s weak magnetism. We also report a measurement of a parity-violating, time-reversal-even electromagnetic contribution to proton structure, referred to in the literature as the proton’s anapole moment.

The weak magnetic moment of the proton, designated as μ_Z , is associated with the interaction due to exchange of the weak neutral Z particle. The weak and electromagnetic forces are related through the mixing angle θ_W , a fundamental parameter of the standard model of electroweak interactions that relates the Z boson to its charged counterparts, the W^\pm (we use $\sin^2 \theta_W = 0.23117 \pm 0.00016$ (6) in our analysis). As a result, one can write μ_Z as

$$\mu_Z = (\mu_p - \mu_n) - 4 \sin^2 \theta_W \mu_p - \mu_s \quad (1)$$

where $\mu_{p(n)}$ are the usual magnetic moments of the proton (neutron) ($2.97\mu_N$ and $-1.91\mu_N$, respectively, where $\mu_N = e\hbar/2m_p = 3.152451238(24) \times 10^{-14}$ MeV-T (6)). The individual contributions of up, down and strange quark-antiquark pairs to the proton’s magnetic moment, μ_u , μ_d , and μ_s , are defined by the relation $\mu_p = \frac{2}{3}\mu_u - \frac{1}{3}\mu_d - \frac{1}{3}\mu_s$. The neutron’s magnetic moment is similarly constructed, interchanging only μ_u and μ_d . Thus, a measurement of μ_Z combined with the known μ_p and μ_n , provides the third observable required to uniquely determine the u , d and s quark pieces of the proton’s magnetic moment. The study of parity-violating electron-nucleon (e - N) scattering enables a determination of the weak magnetic form factor $G_M^Z(Q^2)$, and as a result the equivalent strange piece $G_M^s(Q^2)$,

the momentum-dependent counterpart of μ_Z , where Q^2 is the relativistic four-momentum transferred to the proton by the electron. The Q^2 dependence of these quantities is sensitive to their spatial variation inside the proton.

Whereas the weak magnetism discussed above is a vector e - N interaction, an axial vector e - N coupling also exists, which is related to the proton's intrinsic spin. The parity violating e - p interaction depends on both of these quantities, and it is essential to determine the axial vector e - N form factor G_A^e in order to reliably extract G_M^s . In general, G_A^e may be written as $G_A^e = G_A^Z + \eta F_A + R^e$, where G_A^Z is the contribution from a single Z -exchange as would be measured in neutrino-proton elastic scattering (Fig. 1A), F_A is the nucleon anapole moment (7), and R^e is a radiative correction (Fig. 1C). The constant η is $\frac{8\pi\sqrt{2}\alpha}{1-4\sin^2\theta_W} = 3.45$ where α is the fine structure constant. The anapole moment F_A is identified as the parity-violating coupling of a photon to the nucleon (Fig. 1B) and is expected to be the largest of a class of higher order interactions, or radiative corrections(8). It can arise as a result of, for example, a weak interaction between two quarks inside the nucleon. It is analogous to the nuclear anapole moment recently measured in atomic cesium (9), which is enhanced by parity violating interactions between nucleons in the cesium nucleus (10). Technically, the theoretical separation of the anapole moment from other radiative corrections R^e is gauge dependent, so the terminology associated with these amplitudes varies in the literature, and F_A itself is not cleanly defined theoretically. However, because the anapole moment is an electromagnetic interaction, it does not contribute to neutrino scattering, and is unique to parity-violating interactions with charged particles like electrons. Here we identify the observed difference as due to the anapole contribution (11).

We performed a measurement of the parity violating asymmetry in the scattering of longitudinally polarized electrons from neutrons and protons (nucleons) in deuterium using the SAMPLE apparatus at the MIT/Bates Linear Accelerator Center. The apparatus was that used in our previously reported measurement on hydrogen (4,5). In the deuterium experiment, the hydrogen target was replaced with deuterium, and borated polyethylene shielding was installed around the target to reduce background from low energy neutrons knocked out of the deuterium. Combining this measurement with the previously reported results allows an unambiguous determination of both the axial e - N form factor G_A^e and the contribution of strange quarks to the proton's magnetic form factor G_M^s . When presented in the context of the electron-quark couplings predicted by the standard model for electroweak interactions, our result also places new limits on the electron-quark axial couplings C_{2u} and C_{2d} .

Parity violating electron scattering generally involves scattering of a longitudinally polarized electron beam from an unpolarized target. The change in the count rate resulting from reversal of the beam polarization indicates a parity nonconserving effect. For elastic electron scattering from a proton, the asymmetry in the count rate can be written as

$$A_{PV} = \left(-\frac{G_F}{4\pi\alpha\sqrt{2}} \right) \frac{\varepsilon G_E^p G_E^Z + \tau G_M^p G_M^Z - \varepsilon' (1 - 4\sin^2\theta_W) G_M^p G_A^e}{\varepsilon (G_E^p)^2 + \tau (G_M^p)^2}. \quad (2)$$

The three terms in A_{PV} reflect the fact that it arises as a result of an interference between the electromagnetic and weak interactions, where $G_{E,M}^p$ are the ordinary form factors associated with the proton's charge and magnetic moment. An equivalent expression can be written for

electron-neutron scattering. The kinematic factors $\tau = \frac{Q^2}{4M_p^2}$, $\varepsilon = [1 + 2(1 + \tau) \tan^2(\theta_e/2)]^{-1}$ and $\varepsilon' = \sqrt{(1 - \varepsilon^2)\tau(1 + \tau)}$ can be adjusted to enhance the relative sensitivity of the experiment to the three contributions to A_{PV} .

In the SAMPLE experiment (12), the beam is generated from circularly polarized laser light incident on a bulk GaAs crystal, resulting in an electron beam with an average polarization of 36%. The electrons are then accelerated in durations of 25 μ sec to an energy of 200 MeV before encountering a liquid hydrogen (or deuterium) target. The polarization of the laser light is reversed at the accelerator repetition rate of 600 Hz. After encountering the hydrogen target, the scattered electrons are detected in a large solid angle air Čerenkov detector covering angles between 130° and 170°. Figure 2 depicts 1 of 10 detector modules placed symmetrically about the beam axis. All backward scattered electrons with energies above 20 MeV travel faster than the speed of light in air and generate Čerenkov light that is focussed onto a photomultiplier tube by an ellipsoidal mirror. The integrated photomultiplier current is proportional to the scattered electron rate, which is about 10^8 s^{-1} during the beam pulse. A shutter in front of the photomultiplier tube allows measurement of background coming from neutrons and charged particles. As described in ref. (4), the pulse-height spectrum of the light-producing portion of the signal is characterized with dedicated runs using very low current beam. From these two pieces of information we determine the fraction of the signal due to the Čerenkov yield, which varies from mirror to mirror, but is typically 60%. Several feedback systems are used to minimize the dependence of the properties of the electron beam, such as position, angle and energy, on its polarization state.

The parity-violating asymmetry measured in SAMPLE is dominated by scattering from the neutrons and protons rather than the deuterium nucleus as a whole, and for our incident electron energy of 200 MeV it can be written as

$$A_d = [-7.27 + 1.78G_A^e(T = 1) + 0.75G_M^s] \text{ ppm} \quad (3)$$

(where “ppm” stands for “part per million”). The analogous expression for elastic electron scattering on the proton is

$$A_p = [-5.72 + 1.55G_A^e(T = 1) + 3.49G_M^s] \text{ ppm.} \quad (4)$$

In these expressions we retain explicitly the isovector ($T=1$, or proton – neutron) component of G_A^e . The small isoscalar component (proton + neutron) has been absorbed into the first constant term. The combined measurements allow an independent experimental determination of both quantities.

The raw measured deuterium asymmetry is -1.41 ± 0.14 ppm, with a contribution due to helicity correlated beam parameters of 0.06 ± 0.06 ppm. The measured background contribution to the raw asymmetry is 0.17 ± 0.18 ppm, consistent with zero as expected. The dominant source of background is from photoproduced neutrons, which is known to have a parity-violating asymmetry of less than 1.5% of our measurement (13). In our analysis we assume the background asymmetry is negligible. Removal, on a detector-by-detector basis, of all dilution factors (mostly due to the beam polarization but also from background yields) and application of small corrections for contributing physics processes yields a value for the physics asymmetry of

$$A_d = -6.79 \pm 0.64 (\text{stat}) \pm 0.55 (\text{sys}) \text{ ppm} . \quad (5)$$

The dominant sources of systematic error are the beam parameter corrections (5%), determination of the beam polarization (4%), and determination of the signal-to-background ratio (4%). Uncertainties due to our lack of knowledge of the deuterium nuclear structure are about 3% (14).

Combining this measurement with the previously reported hydrogen asymmetry (5) and with the expressions in equations (3) and (4) leads to the two sets of diagonal bands in Fig. 3. The inner portion of each band corresponds to the statistical error, and the outer portion corresponds to statistical and systematic errors combined in quadrature. Our best experimental value of G_M^s is

$$G_M^s(Q^2 = 0.1) = 0.14 \pm 0.29 (\text{stat}) \pm 0.31 (\text{sys}) . \quad (6)$$

In order to quote a result for the static contribution μ_s it is necessary to know the momentum dependence of G_M^s . We use the calculation of (15), resulting in

$$\mu_s = [0.01 \pm 0.29 (\text{stat}) \pm 0.31 (\text{sys}) \pm 0.07 (\text{theor.})] \mu_N \quad (7)$$

where we have added an additional third uncertainty (theor.) to account for error in the extrapolation coming from the range of the theoretical prediction. Combining this result with the known magnetic moments of the neutron and proton implies that the contribution of strange quarks to the proton's magnetic moment is -0.1 ± 5.1 %.

The allowed region in Fig. 3 also provides a determination of the isovector axial e - N form factor. From a theoretical standpoint, the most uncertain contribution to G_A^e is the anapole term. The dominant contribution is expected to come from Fig. 1A, and at the kinematic conditions of the SAMPLE experiment would result in a value of $G_A^e(T = 1) = -1.071 \pm 0.005$ (6,16). This value is analogous to that which would be measured in neutrino scattering. Anapole effects have been estimated to substantially reduce the magnitude of $G_A^e(T = 1)$ (17), and a recent update of that theoretical treatment yields an expected value $G_A^e(T = 1) = -0.83 \pm 0.26$ (18). This latter value is shown as the vertical band in Fig. 3.

Our experimental result is

$$G_A^e(T = 1) = +0.22 \pm 0.45 (\text{stat}) \pm 0.39 (\text{sys}) \quad (8)$$

indicating that the substantial modifications of G_A^e predicted in (18) are not only present, but with an even larger magnitude than quoted. The deviation of our measured value of G_A^e from -1.071 can be interpreted as a large anapole moment of the nucleon. In the case of cesium, the anapole moment is enhanced by collective nuclear effects that are not present for a single nucleon. Understanding these higher order electroweak processes is essential to reliably interpret precision studies of atomic parity violation and other tests of the electroweak theory.

If further theoretical work fails to produce agreement with this experimental result, it may be necessary to consider the possibility that the discrepancy is due to new physics not contained in the standard model of electroweak interactions. In that regard, we can recast our result in terms of the electron-quark axial coupling parameters C_{2u} and C_{2d} (6).

Present limits on these quantities are from the first parity violating electron scattering experiment (19) and from a measurement performed at the Mainz electron accelerator (20). The form factor $G_A^e(T = 1)$ is related to the combination $C_{2u} - C_{2d}$, resulting in our new experimental value of

$$C_{2u} - C_{2d} = +0.015 \pm 0.032 (\text{stat}) \pm 0.027 (\text{sys}) . \quad (9)$$

This represents a factor of three improvement over the precision of the Mainz measurement. In the Standard Model, the dominant contribution of Fig. 1A would result in

$$C_{2u} - C_{2d} = -(1 - 4 \sin^2 \theta_W) = -0.075 . \quad (10)$$

Adding in the corrections associated with the amplitudes displayed in Figs. 1B and 1C changes the value to -0.058 ± 0.02 . Unless additional contributions to $G_A^e(T = 1)$ are identified that can improve the agreement, our measurement is in disagreement with the present standard electroweak prediction at the 1.5σ level.

An improved determination of G_A^e will be provided with a new measurement of parity-violating quasielastic electron-deuteron scattering at a lower beam energy. The spatial dependence of the strange quark contributions and G_A^e will be studied in detail in an upcoming program of parity violation measurements at the Thomas Jefferson National Accelerator Facility.

References

1. G. Miller, *et al.*, *Phys. Rev.* **D5**, 528 (1972).
2. D. Kaplan, A. Manohar, *Nucl. Phys.* **B310**, 527 (1988).
3. R. D. McKeown, *Phys. Lett.* **B219**, 140 (1989).
4. B. A. Mueller, *et al.*, *Phys. Rev. Lett.* **78**, 3824 (1997).
5. D. T. Spayde *et al.*, *Phys. Rev. Lett.* **84**, 1106 (2000).
6. Particle Data Group, D. E. Groom, *et al.*, *Eur. Phys. J.* **C15**, 1 (2000).
7. I. Zel'dovich, *JETP Lett.* **33**, 1531 (1957).
8. Note that our definition of F_A differs from that used in the atomic physics literature by a factor of $m^2 G_F$ (where $G_F=1.16639(2)\times 10^{-5}$ GeV $^{-2}$ is the muon decay constant and m is the proton mass in units of (GeV/ c^2)), with the result that we expect the value of F_A to be of order unity.
9. C. S. Wood, *et al.*, *Science* **275** 1759 (1997). See also W. Haxton, *Science* **275** 1753 (1997).
10. W.C. Haxton, E.M. Henley, M.J. Musolf, *Phys. Rev. Lett.* **63**, 949 (1989).
11. The contributions to the radiative corrections in parity-violating electron scattering (R^e) compared to neutrino scattering (R^ν) are not quite the same, but the differences are calculated to be small compared to our measurement. Calculations were presented in ref. 16 below, but anapole-type contributions are not specifically identified. For a breakdown into anapole contributions compared with other terms, see M. Musolf, Ph.D. thesis, Princeton University, 1989.
12. The authors here, and those in (4) and (5), constitute the SAMPLE collaboration. As stated in the text, the apparatus used here was identical to that used in (4) and (5) with the exception of the target fluid and some supplementary neutron shielding.
13. T. Oka, *Phys. Rev.* **D27**, 523 (1983).
14. E. Hadjimichael, G. I. Poulis, T. W. Donnelly, *Phys. Rev.* **C45**, 2666 (1992).
15. T. R. Hemmert, U.-G. Meissner, S. Steininger, *Phys. Lett.* **B437**, 184 (1998).
16. A. Liesenfeld, *et al.*, *Phys. Lett.* **B468**, 19 (1999).
17. M. J. Musolf, B. R. Holstein, *Phys. Lett.* **B242**, 461 (1990).
18. S.-L. Zhu, *et al.*, *Phys. Rev.* **D62**, 033008 (2000).
19. C. Y. Prescott *et al.*, *Phys. Lett.* **B84**, 524 (1979).

20. W. Heil *et al.*, *Nucl. Phys.* **B327**, 1 (1989).
21. The skillful efforts of the staff of the MIT/Bates facility to provide high quality beam and improve the experiment are gratefully acknowledged. Supported by NSF grants PHY-9420470 (Caltech), PHY-9420787 (Univ. of Illinois), PHY-9457906/PHY-9971819 (Univ. of Maryland), PHY-9733772 (Virginia Polytechnic Institute) and DOE cooperative agreement DE-FC02-94ER40818 (MIT-Bates) and contract W-31-109-ENG-38 (Argonne National Laboratory), and the Jeffress Memorial Trust (William and Mary, grant no. J-503).

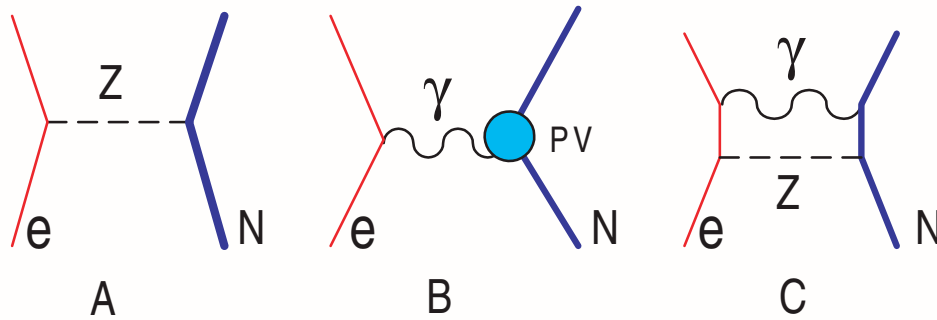


Figure 1

FIG. 1. Feynman diagrams representing three contributions to the axial e - N coupling: A) single Z -exchange, B) parity violating photon exchange, which contributes to the nucleon's anapole moment, and C) a γ - Z box diagram typical of radiative corrections.

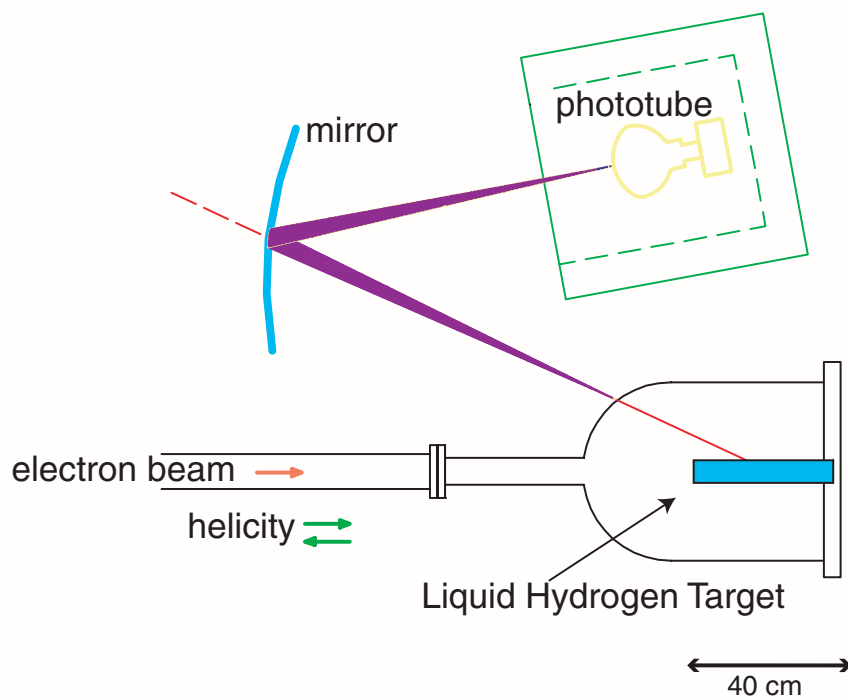


Figure 2

FIG. 2. A schematic view of one module of the SAMPLE experimental apparatus. Ten mirror-phototube pairs are placed symmetrically about the beam axis.

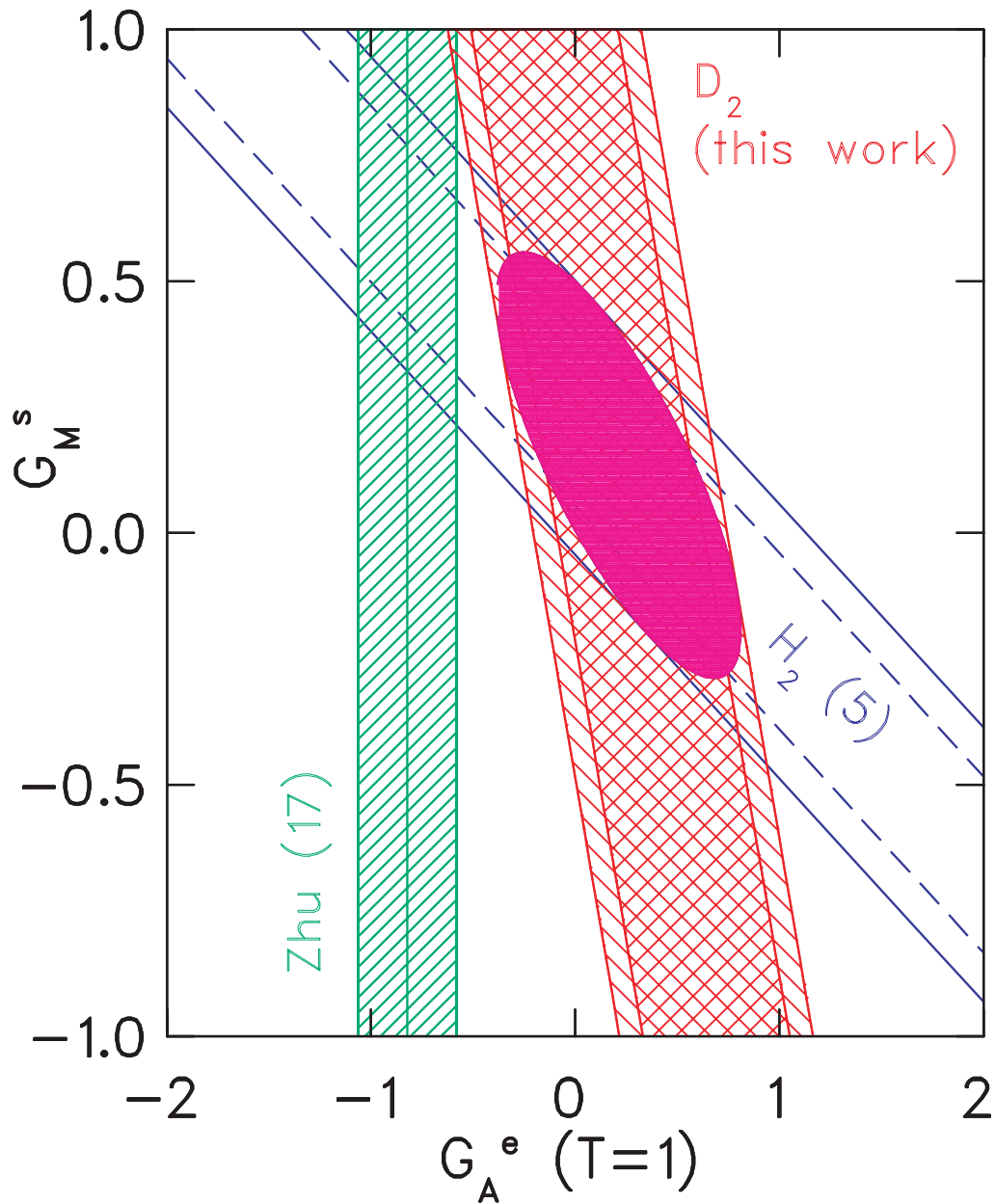


Figure 3

FIG. 3. A result of a combined analysis of the data from the previous two SAMPLE measurements. The two error bands from the hydrogen experiment (5) and the deuterium experiment are indicated. The inner hatched region includes the statistical error and the outer represents the systematic uncertainty added in quadrature. The ellipse represents the allowed region for both form factors at the 1σ level. Also plotted is the estimate of the isovector axial e - N form factor $G_A^e(T=1)$ obtained by using the anapole form factor and radiative corrections of Zhu, *et al.* (13).